AIAA JOURNAL
Vol. 44, No. 6, June 2006

Crushing of a Textile Core Sandwich Panel

Justin Caulfield* and Anette M. Karlsson†
University of Delaware, Newark, Delaware, 19716
and
David J. Sypeck‡
Embry-Riddle Aeronautical University, Daytona Beach, Florida 32114

A class of textile core sandwich structure is investigated with respect to their ability to absorb transverse compressive load. To this end, experimental observations are compared to numerical simulations for cores made from precrimped woven wire cloth laminated together via transient liquid-phase bonding. The experimental observations show that this structure exhibits key properties for being a promising load-absorbing structure, for example, impact and blast protection. Matching numerical simulations show that the behavior can be captured with simulations and that a relatively simplified scheme can be used. The simulations also suggest sensitivity to the local topology in absorbing energy, as well as explaining the somewhat unexpected deformation behavior observed experimentally. Multifunctionality, owing to the accessible open space between cells, coupled with attractive compressive behavior is achieved.

Nomenclature

d	=	diameter of the truss (wire diameter)
E	=	Young's modulus of the material comprising the trusses
G^c	=	shear modulus of the truss core
R	=	radius of the truss, $d/2$
r	=	radius of the connecting element in the woven structure
w	=	opening width (distance between wires)
$\bar{\rho}_{\text{core}}$	=	relative density of the truss core
σ_Y	=	yield strength of the material comprising the trusses
σ_Y^c	=	compressive strength of the truss core
τ_Y^c	=	shear strength of the truss core

I. Introduction

LIGHTWEIGHT metallic materials based on topologically configured cellular trusslike cores and dense face sheets have recently been demonstrated to provide several advantages over competing concepts, such as cores made from more traditional materials such as hexagonal honeycombs or stochastic foams.[1–5] Panels with a stochastic cellular core are not particularly weight efficient.[6] However, panels with periodic truss cores, for example, tetragonal and pyramidal topologies, exhibit superior thermostructural characteristics[3] and are at least as weight efficient as the best competing concepts, for example, honeycombs, especially for curved panels.[6,7] The mechanical benefit from topologically configured cores lies in the ability for individual truss members within the core to absorb external core loads initially as local tensile or compressive truss loads only, with no bending of the trusses. When realized, core properties are related to relative density in a substantially linear way[1–5]:

$$G^c/E = A\bar{\rho}_{\text{core}}, \qquad \tau_Y^c/\sigma_Y = B\bar{\rho}_{\text{core}}, \qquad \sigma_Y^c/\sigma_Y = C\bar{\rho}_{\text{core}} \quad (1)$$

where A, B, and C are a function of truss architecture, load orientation, and node design.

Because of the open space between cells, topologically configured cores provide opportunities for multifunctionality of a structure. For example, a sandwich panel designed for its traditional task (transferring bending moment as coupled pairs in the face sheets and shear stress in the core) could also function as an impact and blast protection device by absorbing loads striking perpendicular to the panel plane. Long, flat stress–strain curves with plastic collapse occurring at a constant (plateau) stress are desired. For trusslike core structures with open interconnected porosity, the aligned channels also provide the needed space for flow of a cooling medium within the structure. This might be advantageous for components subjected to elevated temperatures, for example, hypersonic vehicle airframes, power electronics heat sinks, etc.[5] For a topologically configured core to achieve multifunctional goals at optimum mechanical performance, it is important that the material properties of the base are good, that the nodes (the joints of the trusses) are well designed (to avoid introducing local bending moments into the trusses), and that the trusses adhere nearly perfectly to the face sheets and adjoining trusses.[8–10] However, manufacturing of topologically configured cores with these characteristics can be a challenge from both an economic and technical standpoint.[11]

An alternative and compromise in design criteria and manufacturing techniques for topologically configured materials, for example, honeycombs and cast trusslike structures, involves metallic sandwich panels with textile cores (Fig. 1).[11] This relatively inexpensive approach to fabricating miniature metal trusstype structures[11,12] is based on a recognition that high structural quality porous metal objects have already been made for many years by taking wrought metal wires and weaving them into bundles. Woven wire cloth, braided cables, and knitted metal fabrics are good examples of this.[13] The textile approaches used to create such articles are very well established and relatively inexpensive. Furthermore, a host of base metal choices are available. Virtually all metals can be drawn into wire and then woven, braided, or knitted into a variety of filament arrangements, such as dutch weave, hexagonal mesh, three-dimensional weave, crimped mesh, and triaxial weave.[13]

However, conventional metal textiles are unsuited for most multifunctional applications because the metal contacts are not normally bonded and the articles are thin (exceptions include three-dimensional woven articles). By lamination, many of these shortcomings can be overcome.[11,12] Several base metal types and core architectures have been produced.[12] The aligned porosity provides the open space needed for other functionalities (heat exchange, fuel storage space, conduits for wiring and piping, etc.). Efficient

Received 13 April 2005; presented as Paper 2005-1843 at the AIAA/ASME/ASCE/AHS/ASC 46th Structures, Structural Dynamics, and Materials Conference, Austin, TX, 18–21 April 2005; revision received 7 October 2005; accepted for publication 25 October 2005. Copyright © 2005 by Anette M. Karlsson. Published by the American Institute of Aeronautics and Astronautics, Inc., with permission. Copies of this paper may be made for personal or internal use, on condition that the copier pay the $10.00 per-copy fee to the Copyright Clearance Center, Inc., 222 Rosewood Drive, Danvers, MA 01923; include the code 0001-1452/06 $10.00 in correspondence with the CCC.

*Research Assistant, Department of Mechanical Engineering.
†Assistant Professor, Department of Mechanical Engineering. Member AIAA.
‡Assistant Professor, Department of Aerospace Engineering.

in-plane load support, good mechanical energy absorption, and high convective heat transfer with low pumping requirements have been observed.[11,12,14]

Consider the sandwich structure shown in Fig. 1, where improved shear stiffness and strength (as needed for the cores of sandwich structures subject to bending) can be achieved by having the core porosity take on a diamond-oriented pattern (wires rotated 45 deg within the face sheets). The relative shear stiffness and strength (for bending about the lamination plane) for panels made in this fashion should be about twice that of hexagonal honeycomb because all of the wires get loaded on panel bending (and core shearing) with virtually no wasted material. However, the structure is highly anisotropic. In the following sections, we will investigate a model system based on the diamond-oriented weave to evaluate the crushing performance of this class of system. Experimental investigations will be compared to numerical simulations to illustrate the physical behavior and show that a simplified analysis is possible to estimate the load capacity of this truss core sandwich structure.

II. Experiment

Experimental aspects of the structure being investigated began with precrimped-type 304 stainless-steel wires (diameter $d = 1.2$ mm) woven together forming a distinct squared pattern (opening width $w = 6.4$ mm). The crimps are knuckles in the warp and weft wires that lock the wires into place and are formed with a crimping machine before to weaving. Weaves of this type are advantageous because the wire spacing and amount of wire bending are very accurate and precise. Relatively easy pore alignment for these types of meshes leads to high-quality cellular structures with full nodal contact between laminas, albeit, at additional cost.

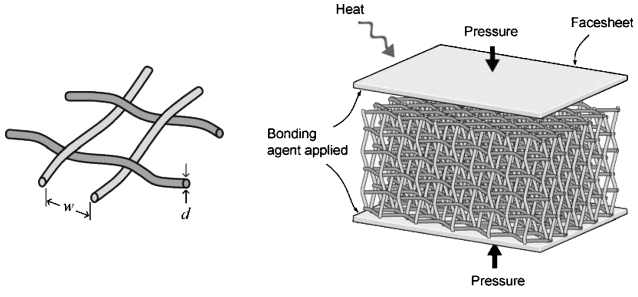

Fig. 1 Unit cell and method for fabricating sandwich structures with textile cores.

To fabricate the cores, the mesh were aligned and laminated (20 ply) together in high vacuum using Ni-25Cr-10P as the transient liquid-phase bonding alloy. Details of this process may be found in Refs. 11 and 12. Two types of structures were made, one with and one without face sheets. The sample without face sheets (Fig. 2) had a height of 53.8 mm, width of 56.2 mm, and thickness of 39.7 mm. The sample with face sheets (Fig. 3) had 57.3 mm (core height = 53.5 mm), 56.2 mm, and 38.0 mm, respectively. The 1.91-mm-thick face sheets were transient liquid-phase bonded in a second heating. The final core relative densities were both 17%. Note that this is a model system to explore the feasibility of the structure. We do not expect that this material system made from steel is in particular suitable for lightweight aerospace structures. When made from more common aerospace alloys such as aluminum and titanium, geometrically identical structures should behave mechanically similar but with properties scaled according to stiffness, strength, and density of the parent alloy.

A convenient way to test the success of the structure is to compress it out-of-plane. Not only is this a relatively simple test method, but it also subjects the core to the most severe loading condition it can experience.[8] For trusslike core structures, experimental results are not readily available in the literature. However, related structures, such as honeycomb[2,15–22] and foam cores[6,23,24] have long been studied for their resistance to compressive loading. Failure always initiates at a local imperfection, commonly leading to the formation of a localized shear band, leading to the final failure.

Both structures were quasistatically compressed to quantify mechanical performance and demonstrate their ability to absorb energy transverse to the primary plane. Eight snapshots of the structure during deformation are shown in Figs. 2 and 3, showing the

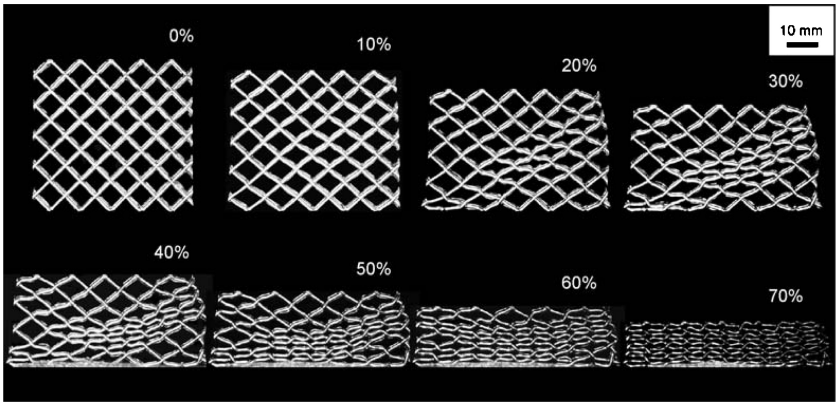

Fig. 2 Deformation during crushing for diamond weave core structure (without facesheets).

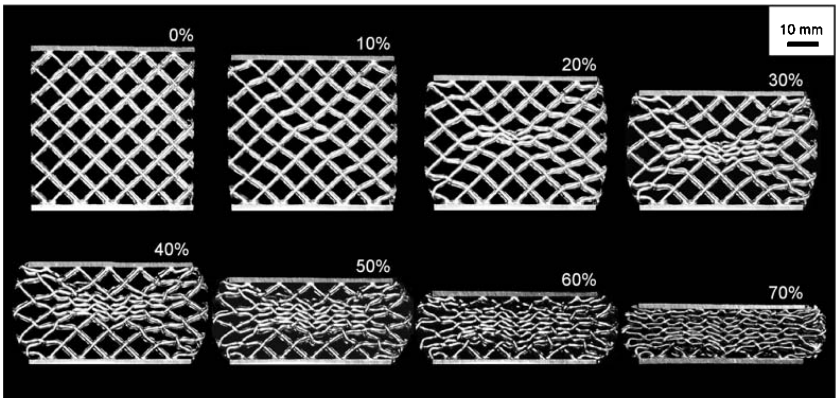

Fig. 3 Deformation during crushing for diamond weave core sandwich structure (with facesheets).

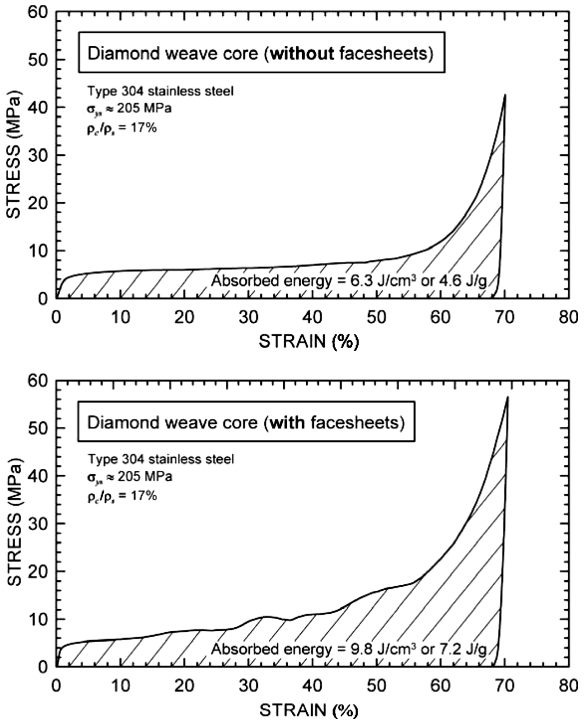

Fig. 4 Stress–strain behavior for diamond weave core structures.

undeformed configuration (0%) and at various stages of compaction up to the maximum deflection (70%). The measured stress–strain curves are presented in Fig. 4. The constitutive responses initially show a small region of near linear-elastic behavior and, thereafter, a region where the stress increases only marginally for increasing strain (more so for the sample with face sheets). This is typical of many cellular solids and shows potential for absorbing large amounts of energy while minimizing and controlling the generated stresses. The initial nonlinear-crushing stress is about 5 MPa for both cases. The sustained crushing stress is about 7 and 10 MPa for the cases without and with facesheets, respectively. Significant strain hardening occurs for the configuration with facesheets. The absorbed energy within the core at maximum strain was 9.8 J/cm^2 (7.2 J/g) for the configuration with face sheets and 6.3 J/cm^2 (4.6 J/g) for the configuration without.

The crushing response depends on the presence or absence of facesheet constraint. When facesheets are present (Fig. 3) the crushing is initiated by collapse of the center diamond followed by the development of deformation bands, stretching from the corners to the center. In the section Numerical Simulations, it will be shown that this is a "global" failure mode, depending on the geometry and boundary only and is not caused by local imperfections.

Absent facesheets to control the deformation (Fig. 2) a localized diagonal shear band of deformed trusses is formed, eventually leading to final collapse of the core. The structure and the load are symmetric. If failure were driven by a global failure mode, as in the case where facesheets are present, the deformation should be symmetric and not localized to an unsymmetric shear band. Thus, the experimental observations imply that failure is governed by imperfections, which could lead to a range of failure modes and deformations depending on defect location, type, and severity. Experimental observations of cellular foam and transversely loaded honeycomb structures show a similar behavior involving localized failure modes. Theoretical investigations designed to help explain these behaviors have shown that failure initiates within the weakest point of the structure, instigating more extensive failure along crush bands.[16,17,24,25]

III. Numerical Simulation

The focus of the numerical simulations is to develop a model that can simulate the compressive behavior for the structure with facesheets. We will not attempt to simulate the behavior for the structure without facesheets (Fig. 2) because it is defect sensitive, not an intrinsic behavior of the structure, and similar behavior has been observed and modeled for related structures.[16,17] In contrast, the failure response for the structure with facesheets (Fig. 3) has not been accurately reported to our knowledge. We will see in this section that the crushing behavior is directly linked to the boundary conditions and the geometry, hence a global structural behavior, and not dominated by imperfections.

To this end, we will explore a simplified method to simulate the response of the structure (without having to model all detailed constituents) and attempt to explain the initiation and evolution of the failure during crushing.

A. Model Definitions

To keep the numerical simulations tractable, we will investigate a two-dimensional system, simulating only one ply of the structure. We will show that this can be sufficient to capture the general behavior of the structure during deformation. Thus, only one layer is simulated. The commercially available finite element program ABAQUS[26] is used.

Two approaches for modeling the woven structure are considered: 1) assume that the nodes meet in one plane, "flat structure," and 2) assume, more accurately, the woven structure where the wires cross with an offset of the dimension of the wire, "woven structure." In the latter case, the (physical) nodes are simulated with a stiff beam element. In addition, two topological configurations are studied: 1) with a diamond in the center (Fig. 5a) and 2) with a nodal point in the center (Fig. 5b). In all cases, three-node beam elements are used to simulate each truss segment. Each physical truss is modeled

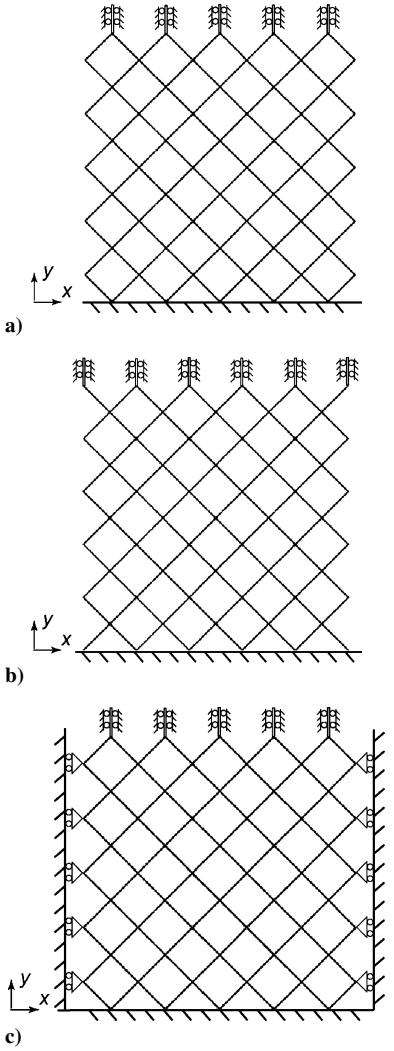

Fig. 5 Models capturing types of morphology and boundary conditions: a) diamond-centered structure, b) node-centered structure, and c) boundary conditions corresponding to infinite structure.

by 25 finite elements, to capture the complicated deformation behavior of the structure. In each case, out-of-plane deformations are prohibited, to simulate the support provided by surrounding plies. The boundary conditions are schematically shown in Fig. 5. The facesheets are considered stiff compared to the structure and are incorporated as boundary conditions (Fig. 5), not modeled explicitly. For comparison, we will also investigate a model corresponding to infinite width or laterally constrained core. To this end, additional side boundary conditions have been included (Fig. 5c).

The model includes the elastic-plastic material properties measured for type 304 stainless steel as used in the testing.[27] This metal exhibits almost linear hardening beyond yield with a 0.2% offset yield strength, $\sigma_y = 217$ MPa. The hardening rate beyond yield can be characterized approximately by a hardening modulus $H = \mathrm{d}\sigma/\mathrm{d}\varepsilon = 2.5$ GPa. Handbook values for this alloy in the annealed condition are $E = 193$ GPa and $\sigma_Y = 205$ MPa (Refs. 11 and 12). The truss diameter is set to 1.2 mm and the opening width to 6.4 mm.

B. Results from Numerical Simulations (with Facesheets)

Qualitatively, models simulating the case with facesheets capture the experimental behavior well, as can be seen by comparing Figs. 6 and 3. For the diamond-centered structure (Figs. 6a and 6b), the deformation is characterized by the center diamond collapsing along with a cross band reaching from each of the four corners toward the center. There is no noticeable difference between the collapse behavior for the flat vs. the woven structure (Figs. 6a and 6b, respectively). The numerical analyses of the node-centered model (Figs. 6c and 6d) show that the diamond above the center node initially deforms at a higher rate than that of the surrounding nodes. As the load increases, adjacent diamonds in the horizontal planes begin to collapse as well. Like the diamond-centered model, differences between flat and woven structures are virtually indistinguishable. Note that at 30% strain, some nodes and elements are above the imaginary line of the upper facesheets (Fig. 6). This is because the facesheets are simulated only by the boundary conditions as shown in Fig. 5. During the actual test (Fig. 3), or if the facesheets had been modeled using a contact analysis, these nodes and elements get pushed down by the facesheets. Thus, this is where the model reaches its limit.

Note that the models do not incorporate the contact between trusses as they collapse onto each other, observed experimentally for deformations higher than 30%. This could be incorporated in the model, but we have omitted that for simplicity at this stage. Hence, we limit the discussion of numerical simulations up to 30% of the total deformation range.

The crushing and instability problem considered here exhibits a special interesting evolution. In traditional instability problems, for example, Euler buckling, a small imperfection needs to be imposed into the finite element model to achieve instability or buckling (unless special routines simulating instabilities are used, of course). However, due to the geometry of this structure, no such imperfection was needed. This is due to the combination of free vertical boundaries in combination with the constraint from the face sheets, as discussed in the analogy discussed in the Appendix. This type of boundary condition compromises the ideal design of a core truss structure, requiring the trusses to absorb a transverse force and bending over the truss at larger deformations. Hence, the trusses will buckle in asymptotic buckling.[28] Numerically, this is possible

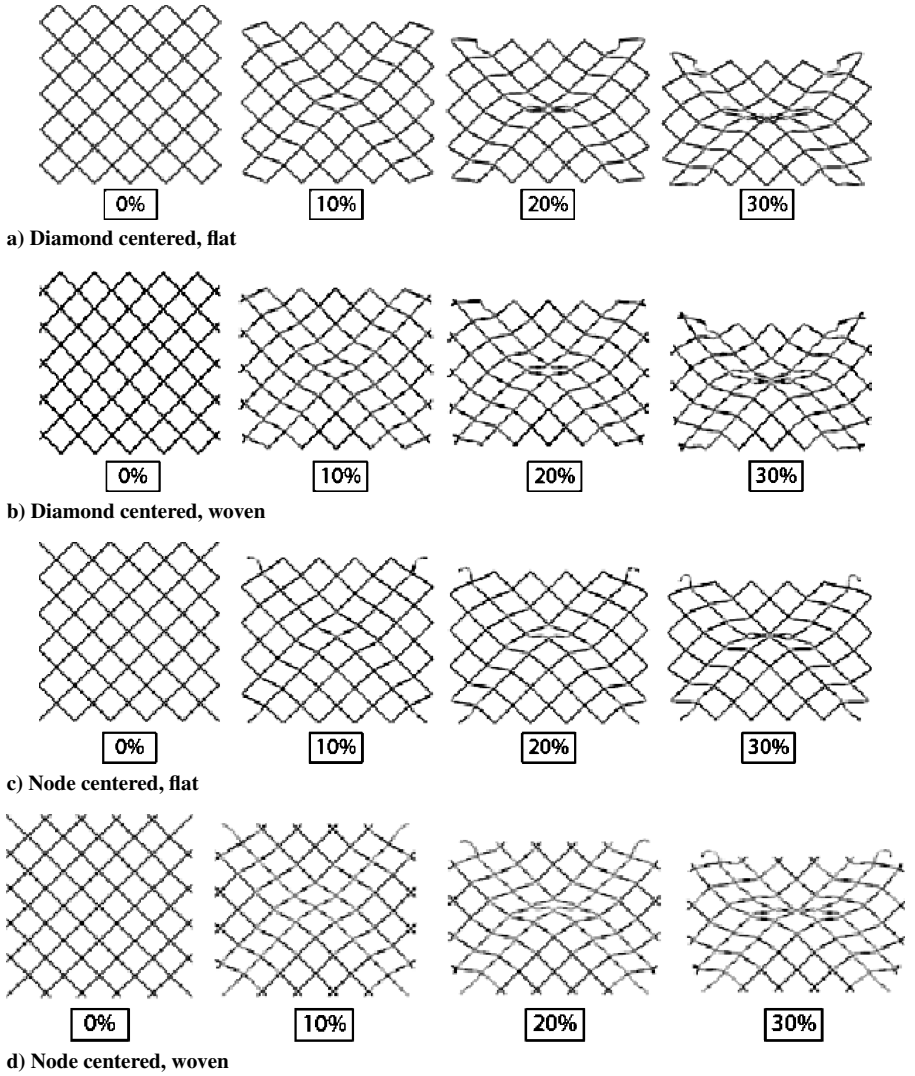

Fig. 6 Evolution of deformation for four models (with facesheets).

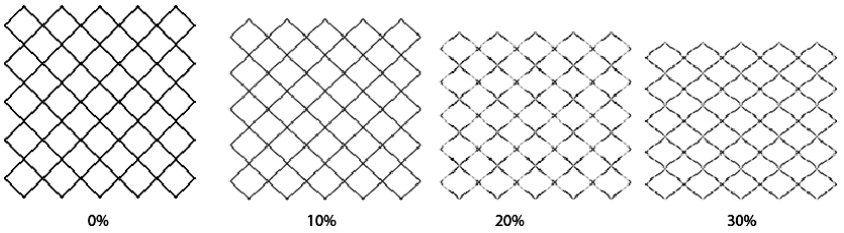

Fig. 7 Evolution of flat, diamond-centered structure with Fig. 5c boundary conditions (with facesheets).

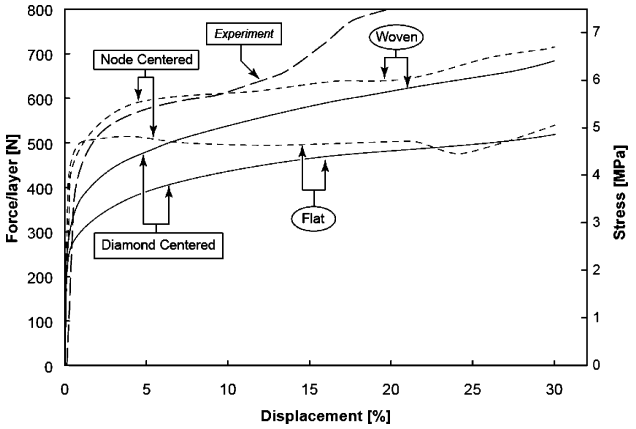

Fig. 8 Force-displacement for four models and comparison to measured data (with facesheets); displacement normalized with initial height.

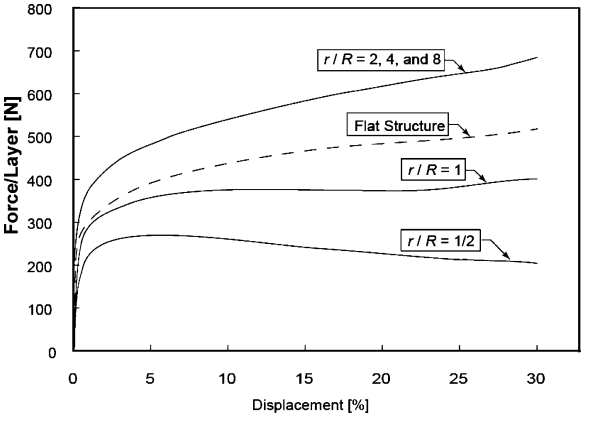

Fig. 9 Force-displacement diagram for various stiffnesses of joints in woven model: diamond-centered woven with facesheets.

because beam elements are used, which indeed can transfer both shear forces and bending moments. For the physical structure, bending of the trusses is possible because the joints between them are stiff and strong enough to absorb a bending moment. Also, the truss will start to yield early during loading and accelerate the bending. Moreover, observe that the overall geometry gives rise to higher stresses in the center of the structure. The stress rising effect can be seen by studying a homogeneous, isotropic squared plate as discussed in the Appendix, where it is seen that the stresses have a local maximum at the center. Thus, for the case where facesheets are present, the geometry lends itself to a stress raiser in the center of the squared structure, serving as a nucleation site for the collapse. As a comparison, consider the situation where the core has a high aspect ratio, namely, where the width is significantly larger than the thickness. The boundary conditions shown in Fig. 5c describe this case, with the results presented in Fig. 7. Thus, this simulates a laterally constrained core with large aspect ratio. Here, the deformation is uniform, and crushing can only be achieved by imposing imperfections, for example, as done by Chung and Waas[11,17] to simulate crushing of a honeycomb core.

The quantitative results are monitored in a force-displacement diagram (Fig. 8). The node-centered models give a stronger response, the nonlinear part of the curve initiates at higher loads compared to the diamond-centered model. This follows directly from the stress-rising effect discussed earlier and in the Appendix. Here, when a centrally located diamond (diamond-centered model) resides at the place of highest stress, the sample begins to collapse at lower loads than the situation when diamonds are located slightly above or below center (node-centered model). However, as the structure is crushed, the response is distinguished by the woven structure exhibiting a higher strain-hardening modulus. Thus, the local topology becomes more important than the overall topology. This may not have been expected, considering that instability problems are imperfection sensitive and that the woven structure simulates the intertwining nature of the wires. However, the modeled woven structure effectively has a stiffer and stronger physical node, reducing the rotation therein, resulting in higher yield strength, plateau stress, and more energy-absorbing response.

The stiffness and strength of the physical node can be changed in the numerical model, by changing the radius of the element connecting the two woven layers (as described in the preceding section). The force-displacement results are shown in Fig. 9, for the diamond-centered, woven case. For Figs. 6–8, the nominal radius r of this element was twice that of the trusses in the structure, R. Using smaller radii for the connecting elements ($r/R = \frac{1}{2}$ and 1, respectively) results in a lower yield strength and plateau stress than that of the flat structure. Interestingly, the stiffness and strength of the connecting beam reaches a saturated value for $r/R \geq 2$, as seen in Fig. 9. Experimentally, this may suggest limits on the amount of bonding agent needed.

Finally, we will quantitatively compare the numerical result to the experiments. The left ordinate in Fig. 8 corresponds to the force required to compress one layer with data directly obtained from the simulations. To compare this to the test results shown in Fig. 4, the corresponding average stress for the structure is exhibited on the right ordinate. In the experiment, stress is determined as measured force divided by sample area (56.2×38.0 mm^2). For the simulations, the equivalent stress is determined by multiplying the individual ply force by the number of ply in the sample (20) and dividing by the area. The results show that the woven structures simulate the experimental results well regarding the initiation of the nonlinear region. However, the numerical simulations tend to underestimate the strain hardening, which is, again, likely due to a weaker simulation of the physical nodes and the omission of contact between the trusses in the numerical model. Nonetheless, when the overall complexity of the deformation is considered, the modeling approach appears to have much merit.

IV. Summary

The crushing of a diamond-weave textile core sandwich panel produced through a novel fabrication technique has been investigated, both experimentally and numerically. This type of structure shows much potential for multifunctional load support. In this study, we have investigated its potential for serving as a panel with enhanced capability for absorbing compressive loads perpendicular to the facesheet plane. Experimental crushing observations show a large region where the response involves nearly constant force during crushing, a key feature for materials suitable for impact and blast protection. The numerical simulations, limited to the case of facesheets, show that the structure can be modeled efficiently by a

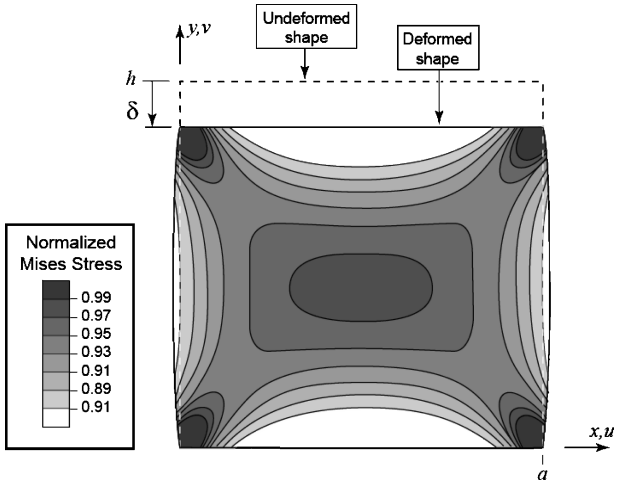

Fig. A1 Stress distribution of squared cross section, subjected to uniform displacement δ.

simplified, two-dimensional approach. The simulation also suggests that perfectly bonded woven structures can potentially absorb more energy than an ideal one-dimensional flat grid structure.

Appendix: Compression of a Solid, Isotropic, Rectangular Plate

Consider an elastic plate of unit thickness with width a and height h. We attach a coordinate system where the x direction spans the width and the y coordinate the height. If the boundary conditions $u(x=0)=0$, $u(x=a)=0$, $v(y=0)=0$, and $v(y=h)=-\delta$, where u and v are the displacement in x and y, respectively, are applied, the stresses σ_{xx} and σ_{yy} in the x and y directions follow directly from Hooke's generalized law:

$$\sigma_{xx} = \xi E(\delta/b), \qquad \sigma_{yy} = \eta E(\delta/b) \tag{A1}$$

where E is the elastic modulus and for plane stress,

$$\xi = \nu\eta, \qquad \eta = 1/(1-\nu^2) \tag{A2a}$$

and for plane strain,

$$\xi = \nu/(1-\nu)\eta, \qquad \eta = (1-\nu)/(1+\nu)(1-2\nu) \tag{A2b}$$

where ν is Poisson's ratio. We note that the stresses are uniform.

When the boundaries conditions are changed so that $u(y=0)=0$, $u(y=h)=0$, $v(y=0)=0$, and $v(y=h)=-\delta$, thus leaving the edges at $x=0$ and $x=a$ free to deform, a closed-form solution cannot be achieved. (No such solution is known to the authors.) The solution from a finite element calculation for these later boundaries is shown in Fig. A1, displaying Mises stresses [normalized with σ_{yy} in Eq. (A1)]. In this case, we have assumed $a=h$. It is evident that the stresses are not uniform. The stress concentration in the corners follows from the boundary conditions. Interestingly, this solution also has a local maximum at the center of the structure. This stress distribution is what we believe causes the failure to initiate in the center diamond (Fig. 3).

Acknowledgment

D. Sypeck gratefully acknowledges support provided by the Embry-Riddle Aeronautical University Research Fund.

References

[1]Wicks, N., and Hutchinson, J. W., "Optimal Truss Plates," *International Journal of Solids and Structures*, Vol. 38, No. 30-31, 2001, pp. 5165–5183.

[2]Wallach, J. C., and Gibson, L. J., "Mechanical Behavior of a Three-Dimensional Truss Material," *International Journal of Solids and Structures*, Vol. 38, No. 40-41, 2001, pp. 7181–7196.

[3]Deshpande, V. S., and Fleck, N. A., "Collapse of Truss Core Sandwich Beams in 3-Point Bending," *International Journal of Solids and Structures*, Vol. 38, No. 36-37, 2001, pp. 6275–6305.

[4]Deshpande, V. S., Fleck, N. A., and Ashby, M. F., "Effective Properties of the Octet-Truss Lattice Material," *Journal of the Mechanics and Physics of Solids*, Vol. 49, No. 8, 2001, pp. 1747–1769.

[5]Evans, A. G., Hutchinson, J. W., Fleck, N. A., Ashby, M. F., and Wadley, H. N. G., "The Topological Design of Multifunctional Cellular Metals," *Progress in Materials Science*, Vol. 46, No. 3-4, 2001, pp. 309–327.

[6]Ashby, M. F., Evans, A. G., Fleck, N. A., Gibson, L. J., Hutchinson, J. W., and Wadley, H. N. G., *Metal Foams—A Design Guide*, Butterworth-Heinemann, Boston, 2000.

[7]Evans, A. G., Hutchinson, J. W., and Ashby, M. F., "Multifunctionality of Cellular Metal Systems," *Progress in Materials Science*, Vol. 43, No. 3, 1998, pp. 171–221.

[8]Hyun, S., Karlsson, A. M., Torquato, S., and Evans, A. G., "Simulated Properties of Kagome and Tetragonal Truss Core Panels," *International Journal of Solids and Structures*, Vol. 40, No. 25, 2003, pp. 6989–6998.

[9]Sugimura, Y., "Mechanical Response of Single-Layer Tetrahedral Trusses Under Shear Loading," *Mechanics of Materials*, Vol. 36, No. 8, 2004, pp. 715–721.

[10]Wang, J., Evans, A. G., Dharmasena, K., and Wadley, H. N. G., "On the Performance of Truss Panels with Kagome Cores," *International Journal of Solids and Structures*, Vol. 40, No. 25, 2003, pp. 6981–6988.

[11]Sypeck, D. J., and Wadley, H. N. G., "Multifunctional Microtruss Laminates: Textile Synthesis and Properties," *Journal of Materials Research*, Vol. 16, No. 3, 2001, pp. 890–897.

[12]Sypeck, D. J., "Constructed Cellular Metals," *Processing and Properties of Lightweight Cellular Metals and Structures*, TMS Conf. Proceedings, TMS, Warrendale, PA, 2002, pp. 35–45.

[13]Ko, F. K., *Textile Structural Composites*, Elsevier, Amsterdam, 1989, p. 129.

[14]Tian, J., Kim, T., Lu, T. J., Hodson, H. P., Queheillalt, D. T., Sypeck, D. J., and Wadley, H. N. G., "The Effects of Topology upon Fluid-Flow and Heat-Transfer Within Cellular Copper Structures," *International Journal of Heat and Mass Transfer*, Vol. 47, No. 14-16, 2004, pp. 3171–3186.

[15]Klintworth, J. W., and Stronge, W. J., "Elasto-Plastic Yield Limits and Deformation Laws for Transversely Crushed Honeycombs," *International Journal of Mechanical Sciences*, Vol. 30, No. 3-4, 1988, pp. 273–292.

[16]Chung, J., and Waas, A. M., "Compressive Response of Honeycombs Under In-Plane Uniaxial Static and Dynamic Loading, Part 1: Experiments," *AIAA Journal*, Vol. 40, No. 5, 2002, pp. 966–973.

[17]Chung, J., and Waas, A. M., "Compressive Response of Honeycombs Under In-Plane Uniaxial Static and Dynamic Loading, Part 2: Simulations," *AIAA Journal*, Vol. 40, No. 5, 2002, pp. 974–980.

[18]Papka, S. D., and Kyriakides, S., "Inplane Compressive Response and Crushing of Honeycomb," *Journal of the Mechanics and Physics of Solids*, Vol. 42, No. 10, 1994, pp. 1499–1532.

[19]Papka, S. D., and Kyriakides, S., "Experiments and Full-Scale Numerical Simulations of In-Plane Crushing of a Honeycomb," *Acta Materialia*, Vol. 46, No. 8, 1998, pp. 2765–2776.

[20]Papka, S. D., and Kyriakides, S., "In-Plane Crushing of a Polycarbonate Honeycomb," *International Journal of Solids and Structures*, Vol. 35, No. 3-4, 1998, pp. 239–267.

[21]Papka, S. D., and Kyriakides, S., "Biaxial Crushing of Honeycombs—Part I: Experiments," *International Journal of Solids and Structures*, Vol. 36, No. 29, 1999, pp. 4367–4396.

[22]Papka, S. D., and Kyriakides, S., "In-Plane Biaxial Crushing of Honeycombs—Part II: Analysis," *International Journal of Solids and Structures*, Vol. 36, No. 29, 1999, pp. 4397–4423.

[23]Gibson, L. J., and Ashby, M. F., "The Mechanics of 3-Dimensional Cellular Materials," *Proceedings of the Royal Society of London, Series A: Mathematical Physical and Engineering Sciences*, Vol. 382, No. 1782, 1982, pp. 43–59.

[24]Bastawros, A. F., Bart-Smith, H., and Evans, A. G., "Experimental Analysis of Deformation Mechanisms in a Closed-Cell Aluminum Alloy Foam," *Journal of the Mechanics and Physics of Solids*, Vol. 48, No. 2, 2000, pp. 301–322.

[25]Zhou, J., and Soboyejo, W. O., "Compression–Compression Fatigue of Open Cell Aluminum Foams: Macro-/Micro-Mechanisms and the Effects of Heat Treatment," *Materials Science and Engineering, A-Structural Materials Properties Microstructure and Processing*, Vol. 369, No. 1-2, 2004, pp. 23–35.

[26]ABAQUS, Software Package, Ver. 6.5, ABAQUS, Inc., Pawtucket, RI, 2004.

[27]Rathbun, H. J., Wei, Z., He, M. Y., Zok, F. W., Evans, A. G., Sypeck, D. J., and Wadley, H. N. G., "Measurement and Simulation of the Performance of a Lightweight Metallic Sandwich Structure with a Tetrahedral Truss Core," *Journal of Applied Mechanics*, Vol. 71, No. 3, 2004, pp. 368–374.

[28]Karlsson, A. M., and Bottega, W. J., "Thermomechanical Response of Patched Plates," *AIAA Journal*, Vol. 38, No. 6, 2000, pp. 1055–1062.

B. Sankar
Associate Editor